

The effect of ultrasonic amplitude on the performance of ultrasonic vibration-assisted EDM micro-hole machining

Peng Zhang

Zhen Yin (✉ yinzhen12@mail.usts.edu.cn)

Suzhou University of Science and Technology

Chenwei Dai

Ziyang Cao

Qing Miao

Kun Zhang

Research Article

Keywords: EDM, Ultrasonic vibration, Micro-hole, Mathematical Model, Numerical simulation, CFD

Posted Date: May 23rd, 2022

DOI: <https://doi.org/10.21203/rs.3.rs-1643822/v1>

License:  This work is licensed under a Creative Commons Attribution 4.0 International License.

[Read Full License](#)

The effect of ultrasonic amplitude on the performance of ultrasonic vibration-assisted EDM micro-hole machining

Peng Zhang¹, Zhen Yin^{1,2*}, Chenwei Dai^{1,2}, Ziyang Cao^{1,2}, Qing Miao^{1,2}, Kun Zhang¹

(1. School of Mechanical Engineering, Suzhou University of Science and Technology, Suzhou 215009, China

2. Suzhou Key Laboratory of Precision and Efficient Machining Technology, Suzhou University of Science and Technology, Suzhou 215009, China)

Abstract

A study on ultrasonic vibration-assisted electrical discharge machining (UVEDM) micro-hole, which mainly includes three key designs, was conducted to improve the machining performance of the electric discharge machining (EDM) micro-holes on TC4 titanium alloy. First, a mathematical model for the velocity of the flow field in the interelectrode gap was established. Consequently, the effect of the presence or absence of ultrasonic vibration on the flow velocity was analyzed. Furthermore, based on COMSOL Multiphysics, the two distributions of the flow field and the debris in the interelectrode gap were simulated and the influence of ultrasonic amplitude on them was analyzed. Finally, the study of UVEDM micro-hole machining with different ultrasonic amplitudes was conducted. The machining performance of the UVEDM micro-hole was found to increase with the increment of the ultrasonic amplitude and the optimal value of 5.22 μm , while the performance decreases when the ultrasonic amplitude goes beyond the optimal value. Compared with EDM micro-hole, the MRR is increased by 2.4 times, and the electrode loss and hole taper are reduced by 56% and 24%, respectively.

Keywords: EDM, Ultrasonic vibration, Micro-hole, Mathematical Model, Numerical simulation, CFD

1 Introduction

With excellent corrosion resistance and high specific strength, titanium alloy Ti-6Al-4V (TC4) is widely used in aerospace, automotive, and medical device applications. However, due to its low thermal conductivity and high toughness, problems (e.g., high cutting forces and severe tool wear) are noted when conventional drilling is used for machining micro-holes in TC4 [1]. Electrical discharge machining (EDM), which is a noncontact machining process using pulse discharge, can remove material by the heat generated between the tool electrode and workpiece electrode regardless of material strength and hardness [3]. Hence, EDM is more suitable for machining micro-holes because no macroscopic mechanical force appears during the process [5]. Nevertheless, the EDM of micro-holes still faces the problems of accumulating debris at the micro-hole bottom, which will produce abnormal discharge like arcing and short circuits, leading to poor shape accuracy and low material removal rate (MRR) [6].

To enhance debris removal efficiency during EDM of micro-holes, applying ultrasonic vibrations to the tool electrode, the workpiece, or the dielectric has continuously attracted widespread attention. During ultrasonic vibration-assisted electrical discharge machining (UVEDM) of micro-holes, several other approaches (e.g., using single-notch electrode [7], helical electrode [8], and planetarily moved electrode [9]) have been taken to improve the machining performance (e.g., efficiency, tool wear, and hole taper). For example, Zhao et al. [7] adopted a single-notch electrode to increase the capacity of debris removal and developed a mathematical model of the dielectric pressure when ultrasonic vibration was applied to the electrode. In addition, they pointed out that higher MRR and smaller electrode wear rate could be achieved with the increase of ultrasonic amplitude. Moreover, Yu et al. [9] effectively reduced the viscous resistance of dielectric by applying both planetary movement and ultrasonic vibration to the

* The e-mail address: yinzen12@mail.usts.edu.cn

electrode, so the debris and bubbles can be easily removed from the discharge gap. Xing et al. [10] investigated the effect of ultrasonic amplitude on the performance of UVEDM micro-hole machining, and the experimental results showed that the higher the ultrasonic amplitude, the higher the MRR and the smaller the electrode wear rate and hole taper.

Directly observing the machining process is difficult in the UVEDM of micro-holes. Therefore, some scholars have used numerical simulation to simulate the variations of the flow velocity and the pressure and debris distribution in the interelectrode gap during micro-hole machining. Liu et al. [11] established a mathematical model of flow velocity to investigate the effects of ultrasonic amplitude, ultrasonic frequency, and aspect ratio of micro-holes on debris distribution and movement using simulation software Fluent. The simulation results prove that electrode vibration is beneficial to remove the debris in the interelectrode gap, which improves the machining performance. Moreover, Li et al. [12] conducted a fluid simulation on the effect of the ultrasonic circular vibration (UCV) electrode on flow field distribution and discharge debris movement. The simulation results show an increase in both the flow velocity and the efficiency of debris removal, which is beneficial to decreasing the abnormal discharge and improving the machining performance of the micro-hole. Mastud et al. [13] investigated the variation of the flow velocity of the dielectric and debris distribution during UVEDM micro-hole arrays machining. The simulation results show that the flow velocity of the dielectric and the efficiency of debris removal increase with an increase in ultrasonic amplitude and ultrasonic frequency. It is an effective method to enhance the machining performance of the micro-hole by improving the efficiency of the debris removal in UVEDM micro-hole machining [14]. The presence or absence of ultrasonic vibration has different influences on the distribution state of the dielectric and the debris. Therefore, exploring the distribution state of the dielectric and the debris in the interelectrode gap is essential.

In this paper, a mathematical model of flow velocity of the dielectric considering electrode vibration is first established. Based on this, the turbulence model will be developed to investigate the flow velocity law, and the debris distribution law with various ultrasonic amplitudes using COMSOL Multiphysics. Finally, experiments are conducted on the machining performance (e.g., MRR, electrode wear, and micro-hole taper) during UVEDM of micro-holes on titanium alloy TC4.

2 Simulation model

2.1 Geometric model

In conventional EDM of micro-holes, the electrode usually just rotates around its axis. However, in this study, an additional axial ultrasonic vibration has been applied to the electrode. During machining, the debris is generated at the bottom of the micro-hole by electric discharge and is then discharged from the interelectrode gap by the dielectric flow. The debris is usually spherical with a diameter ranging from 90 to 180 nm [13]. Thus, in the geometric model of this study, 10^5 spherical debris with an average diameter of 130 nm are considered randomly distributed at the bottom of the micro-holes. The machining process of micro-holes by UVEDM is illustrated in Fig. 1.

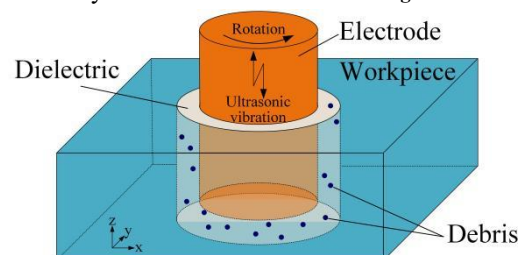


Fig. 1 Schematic diagram of micro-holes machined by UVEDM

Three assumptions have been first put forward before simulation: (a) The dielectric is

incompressible and initially motionless; (b) the process is adiabatic with no thermal exchange or heat dissipate; and (c) the effect of pulse discharge on the flow velocity is not considered.

2.2 Kinematic model of the flow field

In UVEDM of micro-holes, the debris generated in the electrode–workpiece gap is removed due to the drag force caused by the dielectric resistance and the lift force generated by the velocity field of the dielectric^[11]. Hence, the velocity of the flow field significantly affects the removal behavior of debris in processing micro-holes by UVEDM. In this article, both ultrasonic vibration and rotational motion are placed on the electrode. For any point o in the dielectric, the synthesis velocity $v_o(t)$ can be expressed as the vector sum of the vibration velocity $v_1(t)$ and the linear velocity v_2 (Fig. 2). Note that the direction and magnitude of the vibration velocity $v_1(t)$ constantly change with time periodically, and the same is true for synthesis velocity $v_o(t)$. Based on this model, the kinematic models of the flow field under pure electrode vibration and pure electrode rotation are established separately.

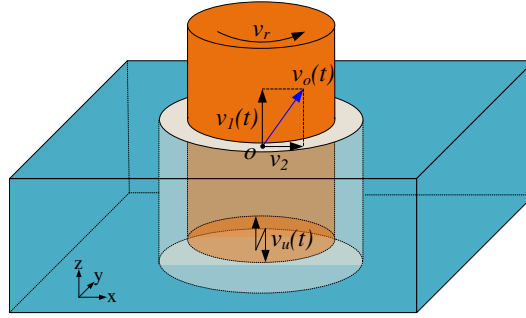


Fig. 2 The composition of velocities.

2.2.1 Processing with pure ultrasonic vibration on electrode

The schematic diagram of processing micro-holes with pure ultrasonic vibration on the electrode is shown in Fig. 3.

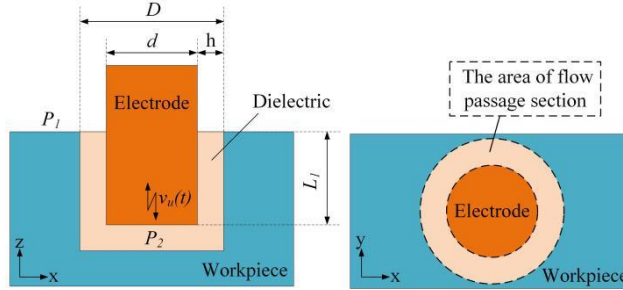


Fig. 3 The schematic of the electrode pure vibration

The electrode vibrates up and down along its axis with the given ultrasonic amplitude A_u and ultrasonic frequency f . Under pure ultrasonic vibration conditions, the electrode trajectory $y_u(t)$, velocity $v_u(t)$, and acceleration $a_u(t)$ can be expressed as:

$$\begin{aligned} y_u(t) &= A_u \sin(2\pi f g) \\ v_u(t) &= A_u g 2\pi f \cos(2\pi f g) \\ a_u(t) &= -A_u g (2\pi f)^2 \sin(2\pi f g) \end{aligned} \quad (1)$$

In the side gap, the velocity of the flow filed $v_1(t)$ can be expressed as^[15]:

$$v_1(t) = \frac{q_1(t)}{A_1} \quad (2)$$

where L_1 is the length of the electrode immersed in the dielectric, q_1 is the flow rate which refers to the volume of liquid passing through the flow passage section per unit time, and A_1 is the area of the flow passage section. Therefore, q_1 and A_1 can be expressed as Eqs. (3) and (**Error! Reference source not found.**), respectively. When the velocity $v_u(t)$ direction is similar to the pressure difference ΔP_1 , a negative sign is used in Eq. (**Error! Reference source not found.**); otherwise, a positive sign is used.

$$q_1(t) = \frac{\pi d h^3}{12 \mu L} \Delta P_1 \pm \frac{v_u(t) \pi d h}{2} \quad (3)$$

$$A_1 = \frac{\pi(D^2 - d^2)}{4} \quad (4)$$

where μ is the viscous resistance of the dielectric, d is the electrode diameter, D is the micro-hole diameter, h is the width of the side gap, ΔP_1 is the pressure difference between inlet pressure P_1 and the bottom pressure P_2 for micro-holes, and the inlet pressure P_1 is zero. Therefore, the pressure difference ΔP_1 could be expressed as Eq. (**Error! Reference source not found.**).

$$\Delta P_1 = P_2 = \frac{a_u(t) g n}{A_e} = \frac{4 a_u(t) g n}{\pi d^2} \quad (5)$$

where A_e is the radial cross-sectional area of the electrode, m is the mass of the free overhanging part (refers to the part from the tip of the horn to the end of the electrode) of the electrode. Thus, the expression of L in Eq. (**Error! Reference source not found.**) is as follows:

$$L = L_1 + A_u \sin(2\pi f g) \quad (6)$$

but L_1 is usually larger than A_u , and L can be considered equal to L_1 .

When the electrode vibrates, the velocity v_i direction is always opposite to that of pressure difference, so the sign in Eq. (**Error! Reference source not found.**) needs to be negative, and Eq. (7) can be obtained by combining Eqs. (1)–(6).

$$v_1(t) = \frac{4}{D^2 - d^2} \left(\frac{a_f(t) g n h^3}{3 \mu L_1 \pi d} - \frac{v_f(t) d h}{2} \right) \quad (7)$$

2.2.2 Processing with pure rotation on the electrode

The geometrical model of the flow field in Fig. 1 is expanded along the circumferential direction and projected onto the XY plane, and the model of the electrode pure rotation in Fig. 4 can be obtained.

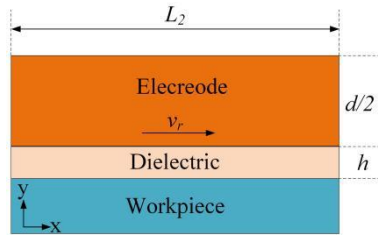


Fig. 4 The schematic of the electrode pure rotation

The above model is a flow field model of the parallel plate, so its flow rate q_2 and area of the flow passage section A_2 can be expressed in Eqs. (**Error! Reference source not found.**) and (**Error! Reference source not found.**)^[15]:

$$q_2 = \frac{L_1 h^3}{12 \mu L_2} \Delta P_2 \pm \frac{L_1 h}{2} v_r \quad (8)$$

$$A_2 = h L_1 \quad (9)$$

where v_r is the linear velocity of the electrode surface, q_2 is the flow rate (refers to the volume of liquid passing through section A_2 per unit time) and A_2 is the area of the flow passage section (refers to the area

of the ring with width h). ΔP_2 in the first term on the right side of Eq. (**Error! Reference source not found.**) is zero and the velocity v_2 of the flow field between the interelectrode gap in the electrode pure rotation can be expressed as Eq. (**Error! Reference source not found.**):

$$v_2 = \frac{q_2}{A_2} = \frac{n\pi d}{2} \quad (10)$$

where n is the rotational speed of the electrode.

In UVEDM micro-hole processing, the electrode has both ultrasonic vibration and rotational motion, so the scalar value of velocity $v_o(t)$ can be expressed as:

$$v_o(t) = \sqrt{[v_1(t)]^2 + v_2^2} = \sqrt{\left[\frac{4}{D^2 - d^2} \left(\frac{a_f(t)gh^3}{3\mu L_f \pi d} - \frac{v_f(t)dh}{2} \right) \right]^2 + \left(\frac{\pi nd}{2} \right)^2} \quad (11)$$

An example calculation of Eq. (11) was performed using MATLAB to find the relationship between ultrasonic amplitude A_u and the velocity $v_1(t)$ of the flow field, where the ranges of the ultrasonic amplitude A_u is from 0 to 10 μm , and the time t is in the range of two cycles of ultrasonic vibration. The remaining variables in Eq. (11) are selected as theoretical values and have no practical significance. The result of the example calculation is shown in Fig. 5.

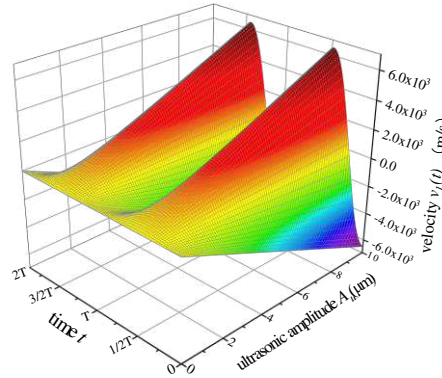


Fig. 5 The relationship between the velocity $v_o(t)$ and the ultrasonic amplitude A_u

The velocity $v_o(t)$ of the flow field increases with the increase of the ultrasonic amplitude A_u (Fig. 5). As time t increases, the velocity $v_o(t)$ of the flow field changes periodically instead of blindly increasing or decreasing.

3. Simulation results and discussion

3.1 Simulation model and boundary condition

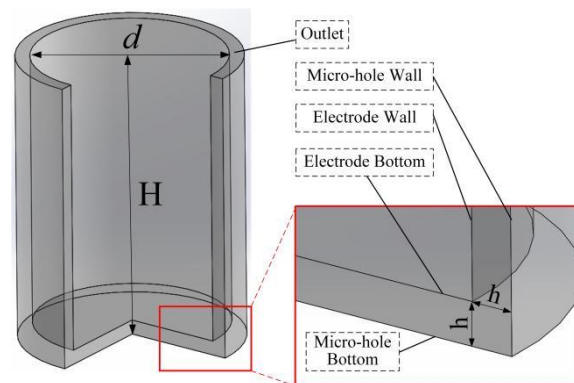


Fig. 6 The three-dimension simulation model

The three-dimension simulation model is shown in Fig. 6. The electrode diameter d and the micro-hole depth H are set at 200 and 300 μm , respectively. The interelectrode gap h plays a crucial role in debris removal and is determined by the four groups of the pre-experiment (the pulse width t_i is 0.6 μs , the pulse

interval t_o is 0.6 μs , the peak current i_e is 6 A, and voltage u_o is 120 V), and the results are shown in Fig. 7.

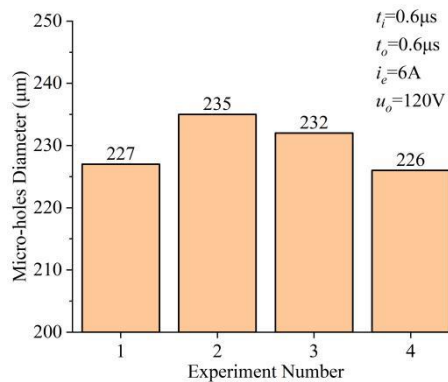


Fig. 7 The results of the pre-experiment

The average of the four micro-hole diameters is 230 μm , therefore the interelectrode gaps (both the side and bottom gaps) are set as 15 μm . The size of the three-dimensional simulation model and other main parameters are listed in Table 1.

Table 1 The size of the three-dimensional simulation model and other main parameters

Items	Values
The density of the dielectric ρ (kg/m^3)	998
Dynamic viscosity of the dielectric μ ($\text{Pa}\cdot\text{s}$)	1.01×10^{-3}
Diameter of the micro-holes D (μm)	230
Diameter of the electrode d (μm)	200
Width of the inter-electrode gap h (μm)	15
The rotational speed of the electrode n (rpm)	240
Ultrasonic amplitude A_u (μm)	0, 1.86, 3.35, 5.22, 8.51, and 13.32
Ultrasonic frequency f (Hz)	43,280

In terms of the physical fields of the fluid flow, the inner surfaces of the model are the electrode wall and the electrode bottom, and all the motion conditions of the electrode will be set on those surfaces. The outer surfaces of the model surface are the micro-hole wall and the micro-hole bottom, and those surfaces will be set on a fixed wall. The ring top of the model is the pressure outlet, which has no velocity inlet and with zero as the initial velocity of the fluid.

In the physical field of particle tracing for fluid flow, the micro-hole bottom is the debris inlet, which is used to generate the debris, and the ring top of the model is the outlet for debris to be discharged from the model, all other walls are set to bounce wall. The debris with a diameter of 90–180 nm occupies the main part of all the debris, and its shape is mostly spherical [13]. To simplify the simulation model, the debris is considered to be spherical with a diameter of 130 nm, and its density is set the 4,510 kg/m^3 similar to that of the TC4 workpiece material. In addition, the debris is randomly distributed at the micro-hole bottom, the number of the debris is set to 10^5 , and the debris velocity is defined as following the flow velocity field.

The debris removal process is divided into two stages: the first stage is the debris removal from the bottom gap of the micro-hole to the side gap and the second stage is the debris removal from the side gap of the micro-hole to the outside. Fig. 8 shows two sections (sections A and B) set on the model shown in Fig. 6. Section A is set at a distance of 7.5 μm from the bottom of the model to determine the working fluid in the bottom gap under different electrode motion states. To accurately observe the law of the changing of fluid velocity with the X - and the Y -coordinates, the flow field distribution is influenced by making two straight lines (lines X and Y) in section A. Section B was set at 150 μm from the bottom of

the model and was used to calculate the number of debris passing through this position under different electrode motion states.

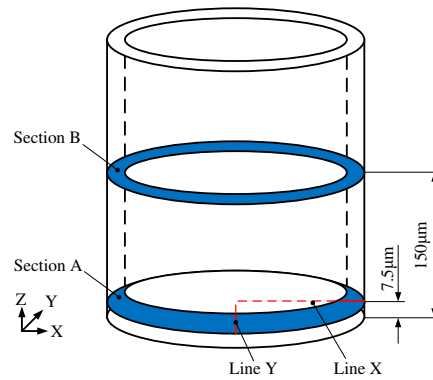


Fig. 8 Schematic diagram of sections A and B

3.2 Effect of ultrasonic vibration amplitude on flow field

The average velocity of the dielectric in the bottom gap is shown in Fig. 9, and the x - and y -direction flow velocities are shown in Fig. 10. Moreover, Fig. 9(a) shows the average velocity under the condition that $A_u = 0$ (the electrode without the ultrasonic vibration) is the smallest in all results and is closely near to 0. Similar results are also shown in Fig. 10(a) and (b). Therefore, removing debris from the bottom of the micro-hole is difficult, which will affect the stability of the micro-hole machining, and it even halts the hole-making processing if the debris accumulates to a certain extent^[12]. Furthermore, Fig. 10(b)–(f) shows that the average velocity increases with the ultrasonic amplitude A_u , and the velocity difference gradually becomes similarly more pronounced. The maximum velocity of the dielectric has appeared at the $1/2$ radius of the micro-hole under the condition that $A_u = 0$, and the maximum velocity only occurs near the micro-hole wall under the condition that A_u is larger than 0 (Fig. 9). In addition, Fig. 10 shows that both the velocity component of the x - and y -directions increase with the ultrasonic amplitude A_u . The greater the ultrasonic amplitude A_u , the larger the maximum flow velocity, and the greater the velocity difference. The debris prefers to move from a low- to a high-velocity area. Thus, the increase of the ultrasonic amplitude A_u is beneficial to debris removal from the micro-hole bottom to the side gap.

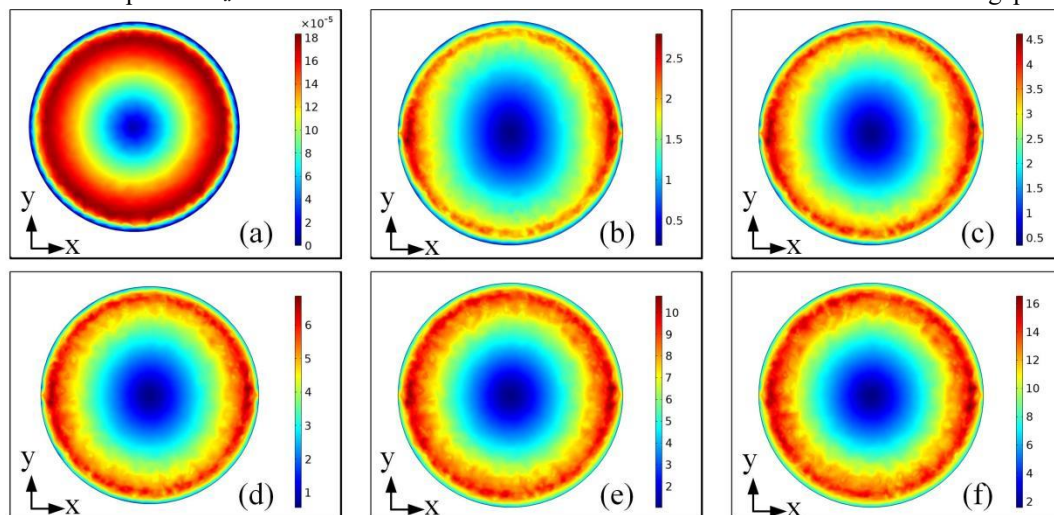


Fig. 9 The average velocity of the dielectric in bottom gap: (a) $A_u = 0 \mu\text{m}$, (b) $A_u = 1.86 \mu\text{m}$, (c) $A_u = 3.35 \mu\text{m}$, (d) $A_u = 5.22 \mu\text{m}$, (e) $A_u = 8.51 \mu\text{m}$, (f) $A_u = 13.32 \mu\text{m}$.

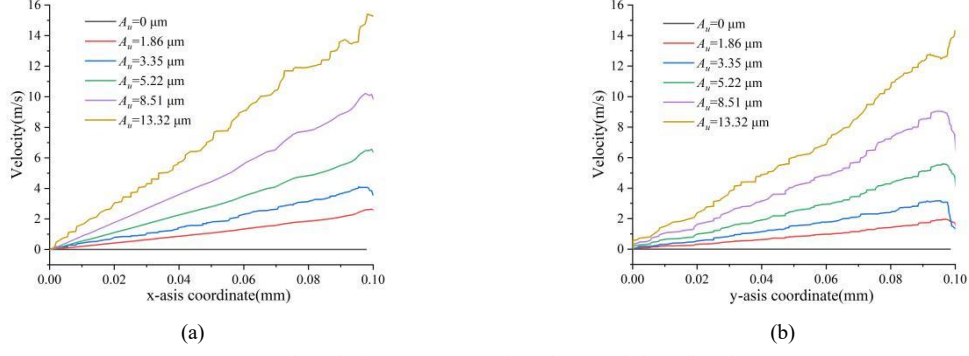


Fig. 10 The velocity component of (a) the x - and (b) y -directions

As the depth of the micro-hole increase, the viscous resistance of the dielectric in the side gap increases gradually, which makes it more difficult to remove debris to the outside^[11]. The high-frequency alternating pressure waves in the dielectric could be generated by the electrode vibration, thereby changing the flow condition of the dielectric and reducing the viscous resistance of the dielectric. The distribution of the flow field in the side gap over time is shown in Fig. 11. The solution time is ten cycles of the ultrasonic vibration, and five cycles of the ultrasonic vibration are selected here. In addition, Fig. 11 shows the velocity and pressure components in the z -direction in the dielectric do not change significantly under the condition of $A_u = 0$, while the value of both is close to 0. Furthermore, Fig. 11(a) shows that the velocity component in the z -direction changes alternately with time, and the velocity amplitude increases continuously with the increase of the ultrasonic amplitude A_u , which is consistent with the results shown in Fig. 5. In addition, the z -direction pressure is shown in Fig. 11(b) and also has similar laws to the velocity component in the z -direction. The ultrasonic vibration not only drastically makes the velocity and pressure of the dielectric change but also effectively facilitate the removal of the debris from the side gap to the outside.

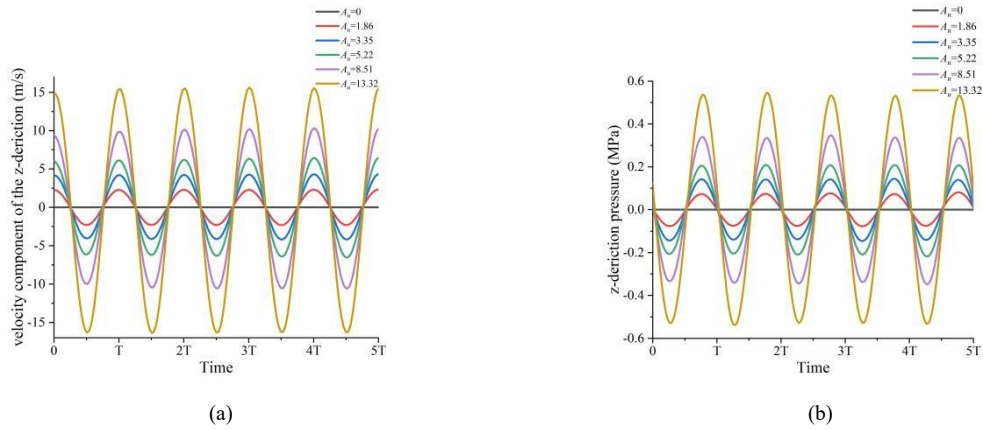


Fig. 11 The distribution of the flow field in side gap over time: (a) the average velocity and (b) the average pressure

3.3 Effect of ultrasonic vibration amplitude on removed debris

In EDM micro-hole machining, too much debris accumulated at the bottom of the micro-hole will cause abnormal discharge, which will not only reduce the machining efficiency but also cause serious electrode wear. The distribution of the debris at two cycles of the ultrasonic vibration ($\sim 46 \mu\text{s}$) under the conditions of different ultrasonic vibrations is shown in Fig. 12. When the ultrasonic amplitude A_u is 0, almost no z -direction velocity exists in the dielectric, which cannot provide sufficient driving force for the debris to be discharged from the side gap to the outside. Thus, the debris is more likely to accumulate at the bottom of the micro-hole, where little debris passes through section B. This will increase the secondary and concentrated discharge at the bottom gap of the micro-hole, thereby reducing the

performance of the micro-hole machining [16]. As the ultrasonic amplitude A_u increases, the number of debris passing through this section increases and reaches a maximum value of 3,332 at $A_u = 13.32 \mu\text{m}$.

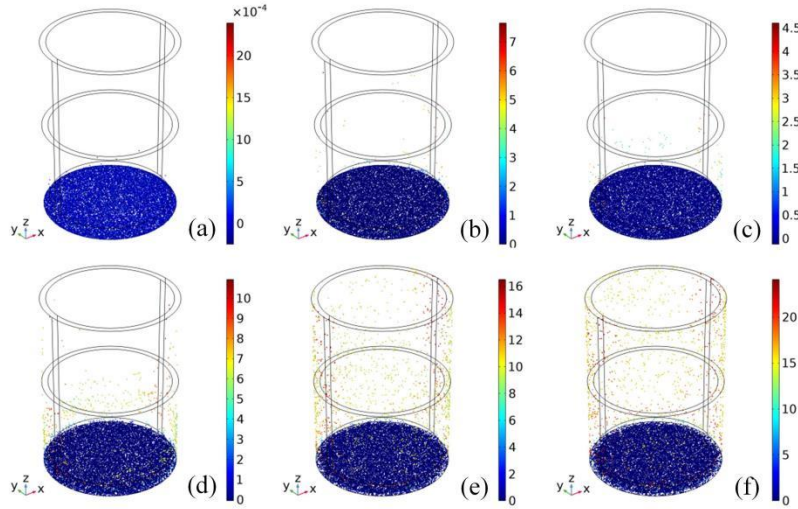


Fig. 12 The distribution of the debris during two ultrasonic vibration cycles under the conditions of (a) $A_u = 0 \mu\text{m}$, (b) $A_u = 1.86 \mu\text{m}$, (c) $A_u = 3.35 \mu\text{m}$, (d) $A_u = 5.22 \mu\text{m}$, (e) $A_u = 8.51 \mu\text{m}$, (f) $A_u = 13.32 \mu\text{m}$.

The number of debris passing through section B under different ultrasonic amplitude A_u is shown in Fig. 13. In the absence of ultrasonic vibration of the electrode, hardly any debris pass through section B. However, Fig. 13 shows that as the ultrasonic amplitude A_u increases, so does the number of debris passing through the section within the same time. The electrode vibration not only increases the pressure difference between the bottom and the side gap of the micro-hole but also increases the velocity component of the z -direction of the dielectric, thereby increasing the amount of debris removal and advancing the debris removal time. In all simulation tests, the number of debris passes through section B when the ultrasonic amplitude is $13.31 \mu\text{m}$ (the largest), which is about 61,000, and the time for the debris to reach section B is about $20 \mu\text{s}$ (the earliest). This indicates that the larger the ultrasonic amplitude, the higher the efficiency of debris removal.

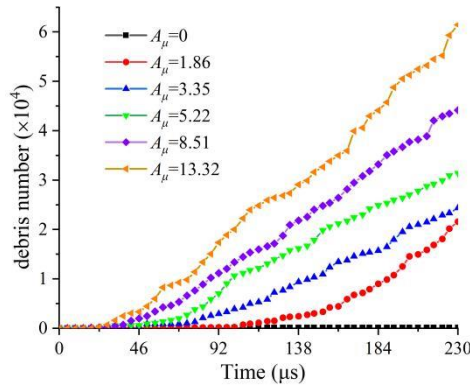


Fig. 13 The number of debris passing through section B under different amplitude A_u

4 Experimental validation

The previous chapter discussed the effect of the ultrasonic amplitude on the flow fluid in the inter-electrode gap, and the simulation results show that increasing the ultrasonic amplitude A_u is beneficial for improving the efficiency of debris removal. To further verify the effect of ultrasonic vibration on EDM micro-hole machining, an experimental study on micro-hole machining under different ultrasonic amplitude A_u will be conducted.

4.1 Experimental details

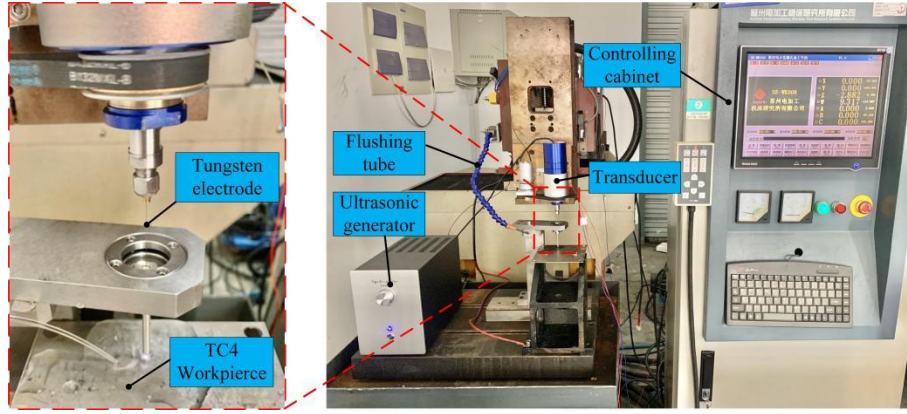


Fig. 14 The UVE micro-hole machining system

The UVE micro-hole machining system in this study is shown in Fig. 14. Taking SE-WK008 EDM micro-hole machine as the basic motion platform, a self-developed ultrasonic transducer is fastened to the vertical column of the micro-hole machine, and the tungsten electrode with a diameter of 200 μm is clamped on the front end of the horn. In the experiment, the method of positive polarity processing was used to process the through holes in the TC4 with a thickness of 2 mm. In addition, the electrical machining parameters (the pulse width t_i is 0.6 μs , the pulse interval t_o is 0.6 μs , the peak current i_e is 6 A, and the voltage u_o is 120 V) during the entire experiment are consistent with that of the pre-experiment. In addition, the electrode wear that the electrode feed stroke is set to 2.7 mm to realize through-hole machining. The working frequency of the transducer measured by the impedance analyzer is 43,280 Hz, and the ultrasonic amplitude under different ultrasonic generator power is measured by the vibrometer (each value is measured four times, and the result is averaged) as shown in Fig. 15. In the experiment, the ultrasonic amplitude is controlled by adjusting the ultrasonic generator power. The detailed experimental parameters are shown in .

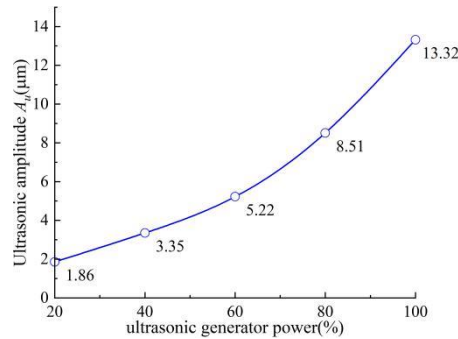


Fig. 15 The ultrasonic amplitude under different ultrasonic generator power

Table 2 Experiment conditions and parameters

Items	Values
Workpiece	100 mm \times 100 mm \times 2 mm, TC4
Electrode	$\phi 180 \pm 5 \mu\text{m}$, tungsten
Dielectric	Deionized water
Electrode feed stroke (mm)	2.7
The rotational speed of the electrode n (rpm)	240
the pulse width t_i (μs)	0.6
the pulse interval t_o (μs)	0.6
the peak current i_e (A)	6
the voltage u_o (V)	120
Ultrasonic frequency f (Hz)	43280

The MRR is directly related to the machining efficiency of the micro-hole. The relative tool wear rate (RTWR) affects the micro-hole accuracy, especially in the blind hole processing. The micro-hole taper θ is one of the important indicators to characterize the shape accuracy of the micro-hole. Therefore, the MRR, RTWR, and micro-hole taper θ are selected to be the evaluation indexes of the machining performance of the micro-hole. The MRR, RTWR, and micro-hole taper θ could be expressed in Eqs. (Error! Reference source not found.)–(Error! Reference source not found.), respectively. Moreover, Fig. 16 is a schematic cross-sectional view of the micro-hole.

$$\text{MRR} = \frac{\pi H (D_{in}^2 + D_{in} D_{out} + D_{out}^2)}{12t} \quad (14)$$

$$\text{RTWR} = \frac{\pi r^2 h / t}{\text{MRR}} \times 100\% \quad (15)$$

$$\theta = \frac{180}{\pi} \arctan\left(\frac{D_{in} - D_{out}}{2H}\right) \quad (16)$$

where D_{in} is the diameter of the micro-hole inlet, D_{out} is the diameter of the micro-hole inlet outlet, H is the micro-hole depth, t is the machining time, r is the electrode radius, and h is the length of the electrode wear.

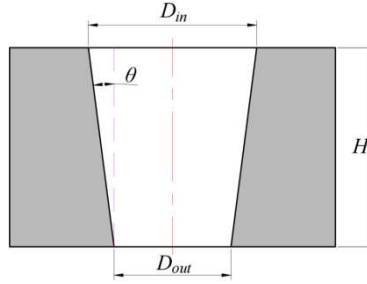


Fig. 16 The schematic diagram of micro-hole cross-section

4.1 Analysis of the micro-hole machining performance

When ultrasonic amplitude A_u is 0 μm , Fig. 17 shows that the MRR is only $1.83 \times 10^5 \mu\text{m}^3/\text{s}$, but the RTWR and micro-holes taper θ are as high as 14.7% and 0.3° , respectively. As the ultrasonic amplitude A_u increases, the MRR increases accordingly and reaches the maximum value of $6.57 \times 10^5 \mu\text{m}^3/\text{s}$ at $A_u = 8.51 \mu\text{m}$, which is 2.6 times higher than the MMR at $A_u = 0 \mu\text{m}$. However, the RTWR reaches the minimum value of 6.5% at $A_u = 5.22 \mu\text{m}$, which is only about half of the RTWR with $A_u = 0 \mu\text{m}$. In addition, Fig. 17(c) shows that when the A_u is larger than 1.86 μm , the micro-hole taper θ is maintained at about 0.2° , and the change in micro-hole taper θ is not significant with the increase of A_u . Based on comprehensive consideration, the micro-hole machining performance with ultrasonic amplitude A_u is believed to be at its best at 5.22 μm .

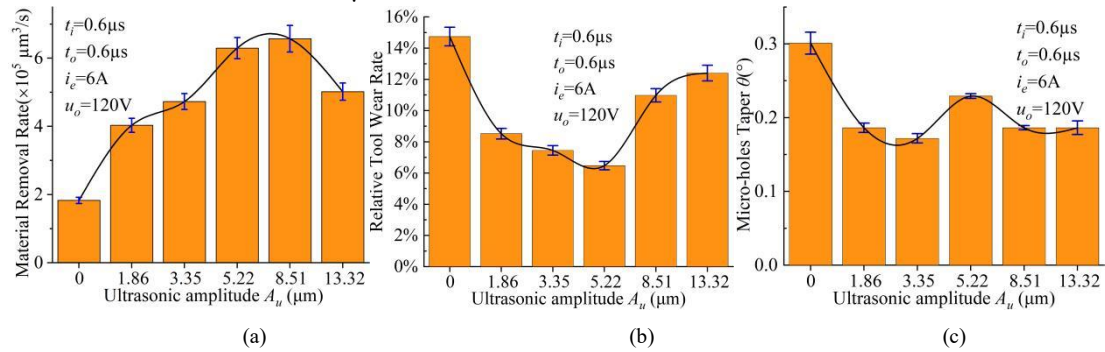


Fig. 17 Effect of the ultrasonic amplitude on (a) MRR, (b) RTWR, and (c) micro-holes taper θ

The simulation results show that the flow velocity and pressure of the fluid in the interelectrode gap are almost zero, so debris can easily accumulate at the bottom of micro-holes, which increases the probability of the abnormal discharge, thereby reducing the MRR and increasing the RTWR. The accumulation of debris at the inlet of the micro-hole causes the probability of the side discharge to increase, so the micro-holes taper θ will also become larger. However, the increase of ultrasonic amplitude A_u can increase the difference in the velocity and pressure of the interelectrode gap fluid, thereby improving the efficiency of debris removal and enhancing the stability of micro-hole machining. The probability of the abnormal discharge and side discharge is reduced, which could increase the MRR and decrease the RTWR and micro-holes taper θ . A decrease in the MRR and an increase in the RTWR with $A_u = 13.32 \mu\text{m}$, which are not in line with the simulation results. In addition, Fig. 18 shows that the worst quality and roundness of the micro-hole inlet are obtained with $A_u = 13.32 \mu\text{m}$.

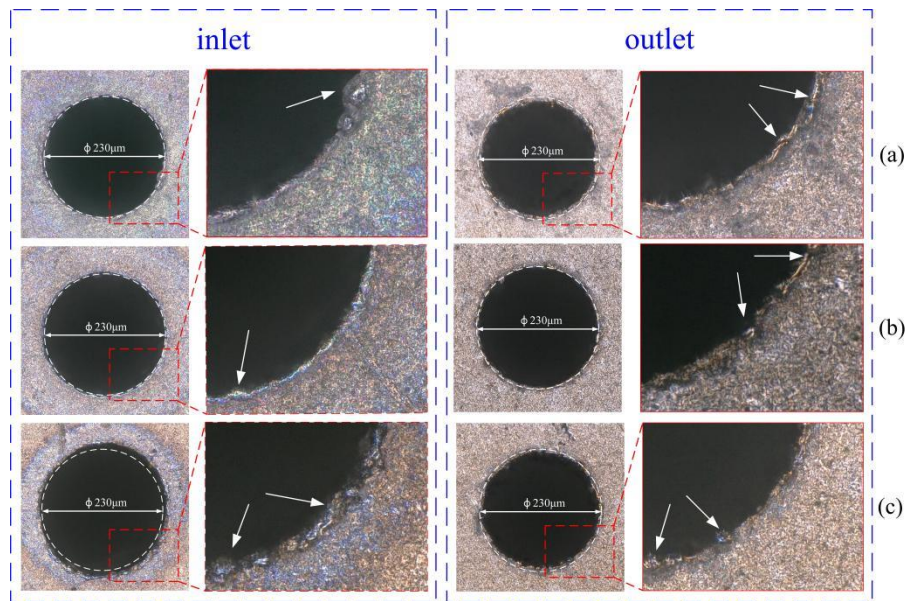


Fig. 18 The micro-hole inlet morphology under ultrasonic amplitude with (a) $A_u = 0 \mu\text{m}$, (b) $A_u = 5.22 \mu\text{m}$, (c) $A_u = 13.32 \mu\text{m}$

Two reasons for the above situation exist. On the one hand, the amplitude at the end of the electrode exceeds the width of the maximum discharge gap, which causes the electrode to contact the workpiece in a very short time, resulting in a short circuit between both [17]. Dong et al. [18] analyzed the situation from the perspective of discharge energy and further explained that when the ultrasonic amplitude is greater than the width of the maximum discharge gap, it will not only cause a short circuit between the electrode and the workpiece. However, the effective discharge energy is greatly reduced, which is the main reason for the lower MRR. On the other hand, when an excessively large ultrasonic amplitude is applied to the slender electrode, it is prone to radial swinging, and then a short circuit between the electrode and the micro-hole wall inevitably occurs. The state is undesirable in EDM micro-hole machining, which not only negatively affects the MRR and the RTWR but also damages the quality of the micro-hole inlet [19]. The frequent contact between the electrode and the workpiece causes the electrode to retreat frequently. Although the retreat time of the electrode is short each time, it still reduces the MRR. In addition, the occurrence of a short circuit between the electrode and the workpiece will also cause the RTWR to increase and the quality of the micro-hole inlet to decrease sharply.

5 Conclusions

The study was conducted to investigate the impact of the ultrasonic amplitude on the performance of EDM micro-hole machining. Under the ultrasonic vibration of the electrode, a mathematical model of the flow field in the interelectrode gap in EDM micro-hole machining was established, and the CFD

simulation of the interelectrode gap fluid was performed. A single-factor experimental study of EDM micro-hole machining under different ultrasonic amplitudes was conducted, which verified the rationality of the results of the mathematical model and the CFD simulation. The main conclusions from this study are as follows:

(1) The flow velocity of the fluid in the interelectrode gap is related to ultrasonic amplitude, ultrasonic frequency, and rotational speed; is not constant when the electrode vibration is used; and alternately changes over time. In addition, the amplitude of the flow velocity also increases with the increase of the ultrasonic amplitude.

(2) The electrode vibration can increase the difference in the flow velocity and pressure of the fluid in the interelectrode gap, and increasing the efficiency of debris removal is also beneficial. Under the condition of ultrasonic amplitude $A_u = 13.32 \mu\text{m}$, the number of chips passing through section B is 61,535. Compared with traditional EDM micro-hole processing, the time for chips to reach section B for the first time is reduced by about 80%.

(3) In this study, the micro-holes machining performance with ultrasonic amplitude A_u is best at $5.22 \mu\text{m}$. Currently, the MRR is increased by 2.44 times, and the RTWR and micro-holes taper θ was reduced by 56% and 24%, respectively, compared with A_u being 0. The excessive ultrasonic amplitude cannot be used in the EDM micro-holes process, otherwise, it will cause some unfavorable factors (e.g., the short circuit between the electrode and the workpiece), which will eventually lead to a decrease in MRR and

Declarations

Funding

The authors gratefully acknowledge the financial support for this work by the National Natural Science Foundation of China (grant no. 51905363), the Natural Science Foundation of Jiangsu Province (grant no. BK20190940 & No. BK20210866), the Natural Science Foundation of the Jiangsu Higher Education Institutions of China (grant no. 19KJB460008 & No. 21KJB460021), the China Postdoctoral Science Foundation (grant no. 2019M661914).

Author Contributions

All authors contributed to the study conception and design. Material preparation, data collection and analysis were performed by [Peng Zhang]. The first draft of the manuscript was written by [Peng Zhang] and all authors commented on previous versions of the manuscript. All authors read and approved the final manuscript.

Consent to participate

It is confirmed that all the authors are aware and satisfied of the authorship order and correspondence of the paper.

Consent for publication

The publisher has the permission of the authors to publish the given article.

Conflict of interest

The authors declare no competing interests.

References

- [1] Mao X, Wang X, Li C, et al. Effects of stepped cylindrical electrode in electrical discharge machining of blind holes(2020). *International Journal of Advanced Manufacturing Technology*, (1): 1457–1469. <https://doi.org/10.1007/s00170-020-05941-3>
- [2] Belloufi A, Mezoudj M, Abdelkrim M, et al. Experimental and predictive study by multi-output fuzzy model of electrical discharge machining performances(2020). *International Journal of Advanced Manufacturing Technology*, 109(7-8): 2065–2093. <https://doi.org/10.1007/s00170-020-05718-8>
- [3] Goigana M, Sarasua J A, Ramos J M. Ultrasonic Assisted Electrical Discharge Machining for High Aspect Ratio Blind Holes(2018). *Procedia CIRP*, 68:81-85. 10.1016/j.procir.2017.12.026
- [4] Pradhan B, Masanta M, Sarkar B, et al. Investigation of electro-discharge micro-machining of titanium super alloy(2009). *International Journal of Advanced Manufacturing Technology*, (41): 1094 – 1106. <https://doi.org/10.1007/s00170-008-1561-y>
- [5] Abu Qudeiri J, Saleh A, Ziout A, et al. Advanced Electric Discharge Machining of Stainless Steels: Assessment of the State of the Art, Gaps and Future Prospect(2019). *Materials*,12(6). <https://doi.org/10.3390/ma12060907>
- [6] Singh P, Yadava V, Narayan A. Machining Performance Characteristics of Inconel 718 Superalloy Due to Hole-Sinking Ultrasonic Assisted Micro-EDM(2018). *Journal of Advanced Manufacturing Systems*, 17(01):89-105. <https://doi.org/10.1142/S0219686718500063>
- [7] Zhao W, Wang Z, Di S, et al. Ultrasonic and electric discharge machining to deep and small hole on titanium alloy(2018). *Journal of Materials Processing Tech*, 120(1-3): 101-106. [https://doi.org/10.1016/S0924-0136\(01\)01149-9](https://doi.org/10.1016/S0924-0136(01)01149-9)
- [8] Hung J C, Lin J K, Yan B H, et al. Using a Helical Micro-tool in Micro-EDM Combined with Ultrasonic Vibration for Micro-hole Machining(2006). *Journal of Micromechanics and Microengineering*,(16): 2705-2713. <https://doi.org/10.1088/0960-1317/16/12/025>
- [9] Yu Z Y, Zhang Y, Li J, et al. High aspect ratio micro-hole drilling aided with ultrasonic vibration and planetary movement of electrode by micro-EDM(2009). *CIRP Annals-Manufacturing Technology*, 58(1): 213-216. <https://doi.org/10.1016/j.cirp.2009.03.111>
- [10] Xing Q, Yao Z, Zhang Q. Effects of processing parameters on processing performances of ultrasonic vibration-assisted micro-EDM(2021). *The International Journal of Advanced Manufacturing Technology*, 112(10): 1-16. <https://doi.org/10.1007/s00170-020-06357-9>
- [11] Liu Y, Chang H, Zhang W, et al. A Simulation Study of Debris Removal Process in Ultrasonic Vibration-assisted Electrical Discharge Machining (EDM) of Deep Holes(2018). *Micromachines*, 9(8). <https://doi.org/10.3390/mi9080378>
- [12] Li Z K, Tang J J, Bai J C.A novel micro-EDM method to improve microhole machining performances using ultrasonic circular vibration (UCV) electrode(2020). *International Journal of Mechanical Sciences*, 175. <https://doi.org/10.1016/j.ijmecsci.2020.105574>
- [13] Mastud S, Kothari N S, Singh R K, et al. Modeling Debris Motion in Vibration-assisted Reverse Micro Electrical Discharge Machining Process (R-MEDM)(2015). *Journal of Microelectromechanical Systems*, 24(3): 661-676. <https://doi.org/10.1109/JMEMS.2014.2343227>
- [14] Zhang Y, Xie B. Investigation on hole diameter non-uniformity of hole arrays by ultrasonic vibration-assisted EDM(2021). *The International Journal of Advanced Manufacturing Technology*, (2). <https://doi.org/10.1007/s00170-021-06597-3>
- [15] Liang, Z Q, Zeng, L W. *Hydromechanics*, Chongqing University Press: Chongqing, China, 2002.

-
- [16] Okada A, Uno Y, Onoda S, et al. Computational fluid dynamics analysis of working fluid flow and debris movement in wire EDMed kerf(2009). *CIRP Annals - Manufacturing Technology*, 58(1): 209-212. <https://doi.org/10.1016/j.cirp.2009.03.003>
- [17] Huang H, Zhang H, Zhou L, et al. Ultrasonic vibration-assisted electro-discharge machining of microholes in Nitinol(2003). *Journal of Micromechanics & Microengineering*, 13(5):693-700. <https://doi.org/10.1088/0960-1317/13/5/322>
- [18] Dong Y, Li G, Wang Y, et al. Study on the effective discharge energy mechanism of vertical ultrasonic vibration-assisted EDM processing(2021).*Proceedings of the Institution of Mechanical Engineers Part B-Journal of Engineering Manufacture*. <https://doi.org/10.1177/09544054211028527>
- [19] Gao C S, Liu Z X. A study of ultrasonically aided micro-electrical-discharge machining by the application of workpiece vibration(2003). *Journal of Materials Processing Tech*, 139(1-3): 226-228. [https://doi.org/10.1016/S0924-0136\(03\)00224-3](https://doi.org/10.1016/S0924-0136(03)00224-3)